SUPPLEMENTAL INFORMATION

Methods

Age model

In the new age model developed for MD04-2845, vegetation-derived climatic phases are correlated with the climate events identified and well-dated in speleothem records (Drysdale et al., 2007). A supplementary control point derives from the correlation of sea surface temperature maximum during the penultimate deglaciation to the likely synchronous highest methane concentration dated in the ice cores (Waelbroeck et al., 2008). Additional control points include MIS boundaries 6/5 and the heaviest values of benthic $\delta^{18}O$ of MIS 6 (Waelbroeck et al., 2008) (Table DR1). From this MD04-2845 age model we inferred ages (indicated as "this work" in Table DR1) for several marine stratigraphic events which were used to establish the chronology of core MD99-2227.

Pollen analysis

Sixty seven samples were analysed for pollen in the interval corresponding to MIS 5 in core MD04-2845 (Fig. DR1). The resolution of the analysis varies between 2 cm and 10 cm, with the highest temporal resolution for the sections corresponding to the LIG (up to 300 years for the beginning of the LIG). The preparation technique follows the protocol established at the UMR EPOC, Bordeaux 1 University (http://www.epoc.u-bordeaux.fr/). The final residue for pollen analysis was mounted unstained in bidistilled glycerine. A minimum of 100 pollen grains, excluding *Pinus*, and 20 pollen morphotypes were counted. Pollen sums including *Pinus* range between 219 and 12,240. The very weak pollen concentrations in several samples of the middle of the LIG from core MD04-2845 result in a lower resolution for this part of the record.

Air temperature reconstructions

Quantitative climatic reconstruction for summer and winter temperature was performed with the Modern Analogue Technique (MAT) (Guiot et al., 1990) (Fig. DR3). The MAT uses the squared-chord distance, effective with percentage data, to determine the degree of similarity between samples with known climate parameters (modern pollen samples) to a sample for which climate parameters are to be estimated (fossil pollen sample). The climate parameter for the unknown sample was calculated as the weighted mean of the closest *n* samples or "analogues". A minimum "analogue" threshold of 8–10 was established beforehand using a Monte Carlo method (Dormoy et al., 2009). If fewer than 8 analogues are found, no climate reconstruction is attempted for that sample. We use a modern pollen dataset that contains more than 3500 modern spectra (lacustrine top-cores including those from large size basins, moss polsters and terrestrial samples) from Eurasia and Northern Africa (Dormoy et al., 2009). The application of the MAT to marine pollen samples has been recently calibrated for the Mediterranean region giving realistic estimations for summer temperature (Combourieu-Nebout et al., 2009).

Sea Surface Temperature reconstruction

Foraminifer assemblages were analysed in the > 150µm fraction of the sediment at a similar resolution to that applied for the pollen counting. Planktonic foraminifera counts were used to perform quantification of Sea Surface Temperatures (SST) by means of an ecological transfer function developed at EPOC laboratory, using the MAT and relying on an extended modern database including the North Atlantic and the Mediterranean basins (1007 points) developed during the MARGO project (Kucera et al., 2005). Modern hydrological parameters were requested on the WOA (1998) database using the tool developed by Schaffer-Neth during the MARGO project (http://www.geo.uni-bremen.de/geomod/Sonst/Staff/csn/woasample.html). Calculations of past hydrological parameters were performed with the R software using a script developed by Guiot and Brewer (www.cerege.fr/IMG/pdf/formationR08.pdf). It relies on a weighted average of SST values from the best five modern analogues, with maximum weight given to the closest analogue in terms of statistical distance / i.e. dissimilarity minimum (Kucera et al., 2005). This method permits the reconstruction of annual and seasonal SST with a degree of confidence (root mean square error) of 1.1°C for spring and annual SST, 1.2 °C for winter and fall SST and 1.3 ° C for Summer SST.

Isotopic analyses

The oxygen and carbon isotope analysis of core MD04-2845 were carried out on *Planulina wuellestorfi* in the fraction above 150 µm following cleaning with distilled water. Each aliquot, including 3-5 specimens and representing a mean weight of 80 µg, was prepared using an automated carbonate preparation device. The extracted CO_2 gas was analysed against NBS 19 standard, taken as an international reference standard. All measurements have been performed using a Delta Plus Finnigan at the LSCE. The mean external reproducibility of powdered carbonate standards is ±0.05‰ for oxygen. Results are presented versus PDB.

Three levels display extremely heavy benthic $\delta^{18}O$ values at the onset of the LIG plateau. None of the $\delta^{18}O$ profiles from the eastern North Atlantic discussed in this work show such a reversal in the oxygen isotopic values (Fig. DR2). We believe, therefore, that these biased values at the Bay of Biscay site are the results of local processes affecting the benthic foraminifera during the penultimate deglaciation.

Model simulations

In all simulations the ice sheet configuration and the sea level stand are fixed at pre-industrial values. To represent the whole range of possible melting scenarios of the GIS in the simulations, the sensitivity experiments include different multiples of the freshwater flux of 0.013 Sv (0.0065 to 0.117 Sv) (Table DR3). The simulations have been run for only 500 years in order not to add too much freshwater to the ocean with respect to the estimated difference between the present and 130 ka volume of the GIS. Although near-equilibrium is not likely to be reached under the influence of a continuous freshening of the ocean, North Atlantic deep water (NADW) export at 30°S reaches quasi-stable levels after about 200 years (Fig. DR5). Because surface properties tend to be highly variable, the NADW is taken as an indicator of the state of the climate.

References

Combourieu Nebout, N., Peyron, O., Dormoy, I., Desprat, S., Beaudouin,C., Kotthoff, U., and Marret, F., 2009, Rapid climatic variability in the west Mediterranean during the last 25 000 years from high resolution pollen data: The Climate of the Past, v. 5, p. 503-521.

Dormoy, I., Peyron, O., Combourieu Nebout, N., Goring, S., Kotthoff, U., Magny, M., and Pross, J., 2009, Terrestrial climate variability and seasonality changes in the Mediterranean region between 15000 and 4000 years BP deduced from marine pollen records: The Climate of the Past, v. 5, p. 615-632.

Drysdale, R.N., Zanchetta, G., Hellstrom, J.C., Fallick, A.E., McDonald, J., and Cartwright, I., 2007, Stalagmite evidence for the precise timing of North Atlantic cold events during the early last glacial: Geology, v. 35, p. 77-80.

Guiot, J., 1990, Methodology of the last climatic cycle reconstruction from pollen data: Palaeogeography, Palaeoclimatolology, Palaeoecology, v. 80, p. 49-69.

Kucera, M., Rosell-Melé, A., Schneider, R. Waelbroeck, C., and Weinelt, M., 2005, Multiproxy approach for the reconstruction of the glacial ocean surface (MARGO): Quaternary Science Reviews, v. 24, p. 813-819.

Lourantou, A. Chappellaz, J., Barnola, J.-M., Masson-Delmotte, V., and Raynaud, D., 2010, Changes in atmospheric CO_2 and its carbon isotopic ratio during the penultimate deglaciation: Quaternary Science Reviews, v. 29, p. 1983-1992.

Pons, A., Guiot, J., de Beaulieu, J. L., and Reille, M., 1992, Recent contribution to the climatology of the last Glacial-Interglacial cycle based on French pollen sequences: Quaternary Science Reviews, v. 11, p. 439-448.

Waelbroeck, C., Frank, N., Jouzel, J., Parrenin, F., Masson-Delmotte, V., Genty, D., 2008, Transferring radiometric dating of the last interglacial sea level high stand to marine and ice core records: Earth and Planetary Science Letters, v. 265, p. 183-194.

Figure DR1

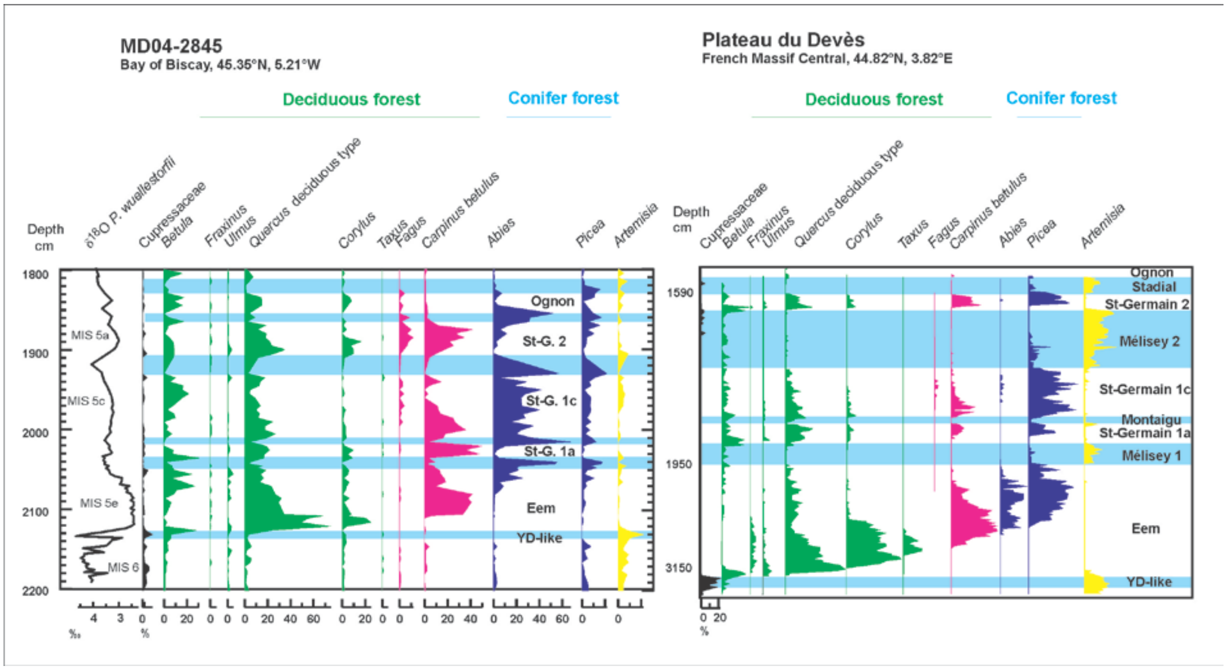

Figure DR1 –High-resolution pollen diagram from the Bay of Biscay core, recruiting pollen from western France mainly through the Garonne (Pyrenees) and Loire (Massif Central) rivers, and its comparison with the terrestrial pollen sequences from the Plateau de Dévès (Massif Central) (Pons et al., 1992). Both records show the same alternation of warm (Eem, St-Germain 1a, St-Germain 1c, St-Germain 2 and Ognon interstadials) and cold (YD-like,Melisey 1, Montaigu, Mélisey 2 and Stadial) phases. Younger Dryas (YD)-like event is related to the stagnation of the temperate forest development and the sharp increase in steppe plants. The subsequent cold episodes are mainly marked in the Bay of Biscay record by the expansion of the Conifer forest (*Abies* and *Picea*) while the concomitant expansion of steppe elements is observed at the high altitudes of the French Massif Central and near the moraines of north eastern France and the Alps (Pons et al., 1992), indicating that these cool-loving trees dominated the low altitudes of western France during the cold episodes of MIS 5.

Table DR1

Event stratigraphy	ka		MD04-2845 Depth (cm)	MD99-2227 Depth (cm)
Top Montaigu (GS 24, C23)	102.6±0.8	Drysdale et al. 2007	2010	
MIS 5d/5c	104.6	This work	2016	1780
Top St Germain 1a	105.1±0.9	Drysdale et al. 2007	2017	
Top Mélisey 1	108.8±1.0	"	2035	
Top Eemian	112±0.8	"	2045	
MIS 5e/5d	120	This work	2078	1840
~base Eemian (SST increase)	131.2±2.0	Waelbroeck et al., 2008	2125	
end H11	132.08	This work	2140	2018
MIS 6/5 (onset H11)	135	Waelbroeck et al., 2008	2160	2028
upper MIS6	141	"	2165	2130

Table DR1 – Age control points for cores MD04-2845, and MD99-2227. C25 and C24: marine cold events; GS: Greenland Stadial, GI: Greenland Interstadial.

Figure DR2

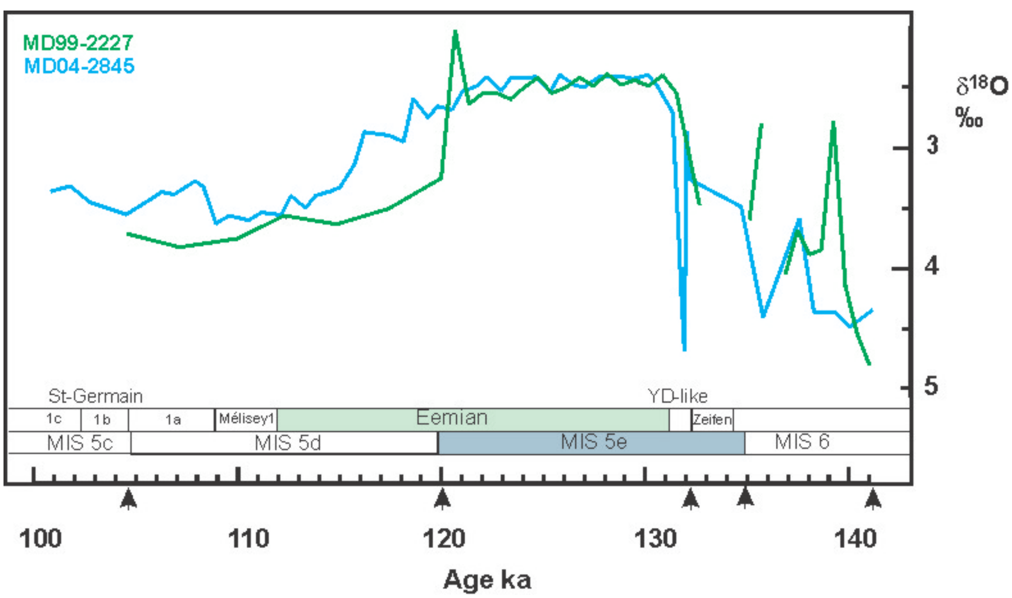

Figure DR2 - Foraminifera δ^{18}O curve of cores MD04-2845 (*P. wuellestorfi*, blue) and MD99-2227 (*N. pachyderma* (s), green). Control points underpinning the common age model between MD04-2845 and MD99-2227 are indicated by arrows.

Figure DR3

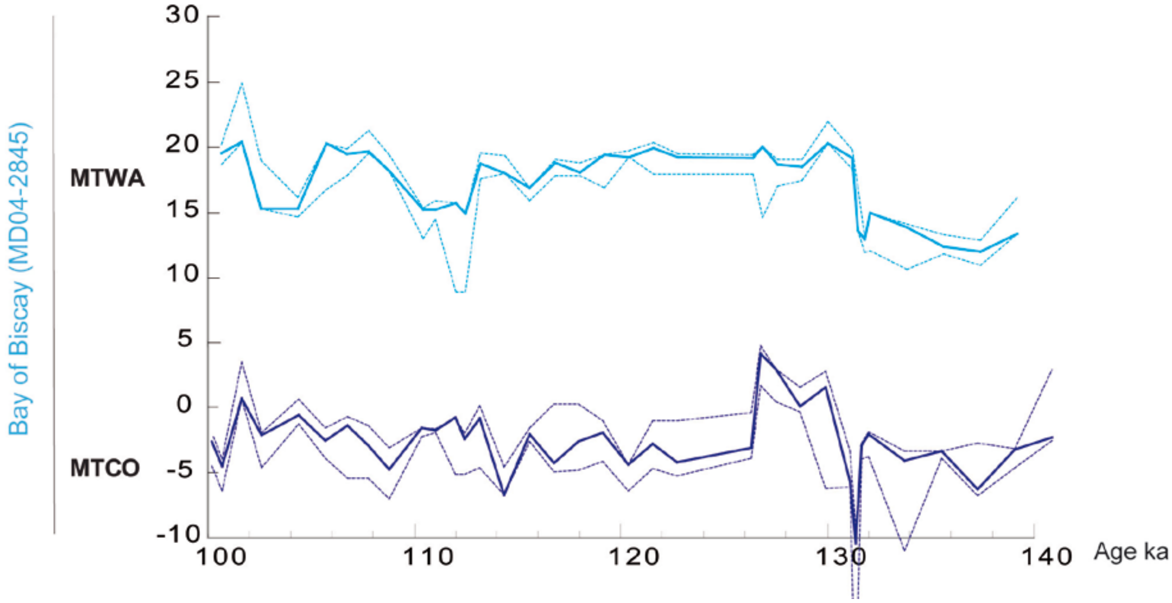

Figure DR3 - Pollen-derived quantitative climate reconstructions with the associated errors for the Mean Temperature of the Warmest (MTWA) and Coldest (MTCO) months in °C.

Figure DR4

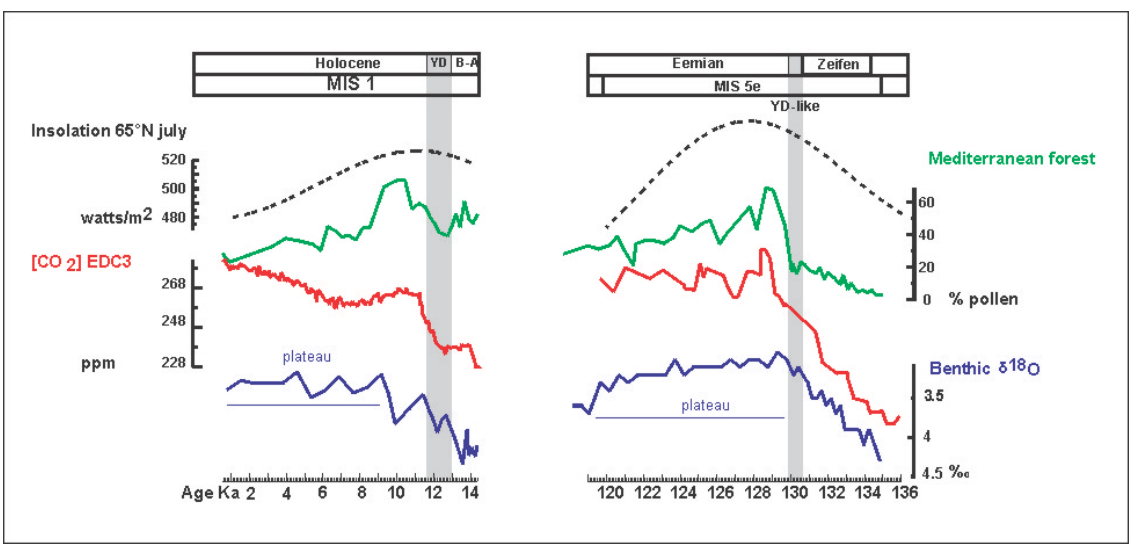

Figure DR4 - Comparison of the timing and amplitude of the pollen inferred-forest cover increase between the Holocene and the LIG in core MD95-2042 (southwestern Iberian margin). Changes in insolation and CO_2 concentration are also shown (Lourantou et al., 2010). The difference in the timing and amplitude of forest development between the Eemian and the Holocene is also suggested by other European pollen sequences (e.g. Plateau de Dévès) (Pons et al., 1992).

Table DR2

Additional freshwater from GIS melting (sV)		0.0065	0.013	0.026	0.039	0.052	0.065	0.078	0.091	0.104	0.117
Anomaly of maximum meridional overturning streamfunction in the North Atlantic (Sv)	Average	-1.534	-2.433	-3.664	-5.388	-8.782	-9.258	-9.787	-10.625	-10.961	-11.983
	2σ	2.144	1.124	0.753	0.728	0.546	0.369	0.498	0.442	0.512	0.443
Anomaly of maximum meridional overturning streamfunction in the GIN Seas (Sv)	Average	0.041	0.068	0.168	0.194	0.177	0.106	0.037	-0.164	-0.144	-0.372
	2σ	0.197	0.195	0.113	0.201	0.235	0.156	0.223	0.335	0.209	0.218
Anomaly of meridional heat flux in the Atlantic Ocean at 30°S (PW)	Average	-0.022	-0.023	-0.031	-0.048	-0.096	-0.105	-0.115	-0.141	-0.147	-0.162
	2σ	0.022	0.038	0.024	0.039	0.037	0.031	0.035	0.022	0.028	0.035
Anomaly of the sea ice area Northern hemisphere ($10^{12}km^2$)	Average	0.007	0.102	0.136	0.213	0.814	0.937	0.958	1.073	1.055	1.218
	2σ	0.172	0.141	0.206	0.191	0.356	0.215	0.310	0.217	0.314	0.323
Anomaly of southwestern European July temperatures (°C)	Average	0.147	-0.073	-0.061	-0.125	-0.349	-0.559	-0.453	-0.656	-0.742	-0.810
	2σ	0.050	0.250	0.565	0.354	0.555	0.407	0.689	0.301	0.479	0.668

Table DR2 - The influence of different freshwater forcing scenarios on North Atlantic climate properties. For the different freshwater forcing scenarios the average anomaly from the 130ka reference simulation and the 96% confidence interval are listed for different important climate properties. These are from top to bottom: the maximum meridional overturning stream function (Sv) in the North Atlantic; the maximum meridional overturning streamfunction (Sv) in the GIN Seas; meridional heat flux in the Atlantic Ocean at 30°S (10^{15}W); Northern hemisphere sea-ice area ($10^{12}km^2$); south-western European July temperatures (^oC). Although it might be suspected that the impact of reduced meridional heat transport by the North Atlantic Drift is greatest on winter month temperatures, differences turned out not to be significant at a 96% confidence level. South-western Europe is defined as the land surface between 37° and 41°N and 0° to 10°W. The average anomaly and 96% interval is calculated after applying a 10 year running mean. A 10 year running mean was chosen in order to filter out all sub-decadal variability. Averages were calculated over the last 150 years of the simulations. Reference values are (in same order as in table): 22.481Sv; 2.690Sv; 0.300PW; 8.280 $10^{12}km^2$; 28.940 ^oC.

Figure DR5

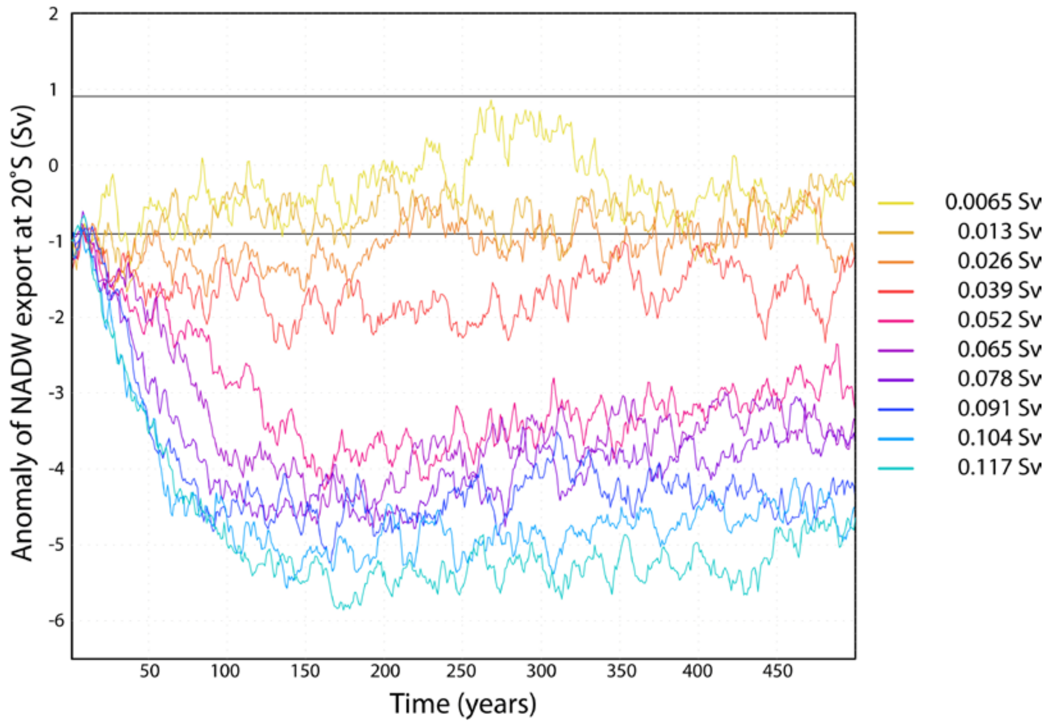

Figure DR5 - Simulated 10 year running mean anomalies of the North Atlantic Deep Water (NADW) export at 20°S (Sv) as a function of time (years). Colours indicate different scenarios with the following amounts of additional freshwater from Greenland Ice Sheet melting: 0.0065Sv (light yellow); 0.013Sv (dark yellow); 0.026Sv (orange); 0.039Sv (red); 0.052Sv (magenta); 0.065Sv (purple); 0.078Sv (dark purple); 0.091Sv (dark blue); 0.104Sv (medium blue) and 0.117Sv (light blue). The reference value is an average over the last 500 years of the 130ka simulation without additional freshwater forcing. The variability in this reference simulation is indicated by the two horizontal black lines depicting the 96% confidence interval (2σ=0.904 Sv) which is calculated after a 10 year running mean has been applied. A 10 year running mean was chosen in order to filter out all sub-decadal variability.